

# Quantum entanglement and drifting generated by an ac field resonant with frequency-doubled Bloch oscillations of correlated particles

W. S. Dias, F. A. B. F. de Moura, and M. L. Lyra\*

*Instituto de Física, Universidade Federal de Alagoas, 57072-900 Maceió-Alagoas, Brazil*

(Received 28 July 2015; published 16 February 2016)

We study the dynamics of initially localized and uncorrelated two-particle quantum wave packets evolving in a one-dimensional discrete lattice. In particular, we show that the particles become strongly entangled when directed by a harmonic ac field which is resonant with frequency-doubled Bloch oscillations promoted by a static dc field. Some degree of entanglement is also achieved when the ac field is resonant with the single-particle Bloch oscillations. However, in this case, entanglement is strongly limited by the survival of anticorrelated unbounded states. We further show that the drift velocity of the correlated-particle wave-packet centroid depends on the phase of the ac field. This dependence is similar to the semiclassical prediction for single-particle motion. The drift velocity vanishes in the limit of uncorrelated particles, as well as for Fock-like initial states, which have a null expectation value of the kinetic operator. We reveal that the interparticle interaction influences unbounded- and bounded-state components differently. This leads to a nontrivial nonmonotonic dependence of the drift velocity on the interaction strength.

DOI: [10.1103/PhysRevA.93.023623](https://doi.org/10.1103/PhysRevA.93.023623)

## I. INTRODUCTION

Recent experiments investigating the behavior of a few interacting atoms in optical lattices [1] opened the possibility of generating a variety of quantum entangled matter states, which could have a great impact on the search for universal and more efficient quantum computation processes, quantum sensing, and metrology [2–4]. It has been experimentally demonstrated that quantum entangled atom pairs perform Bloch oscillations (BOs) at twice the fundamental frequency in tilted optical lattices [1]. BO is the phenomenon of oscillatory motion of wave packets placed in a periodic potential when driven by a constant force [5,6]. It has been observed in several physical contexts such as semiconductor superlattices [7,8], ultracold atoms [9–14], and optical [8] and acoustic [15] waves. The coherent phenomenon of frequency doubling of BOs was predicted to occur in the presence of interaction [16–20] because two particles bind together and perform correlated tunneling. Fractional BOs at multiples of the fundamental BO frequency have also been demonstrated for larger clusters of interacting particles [21]. It has also been theoretically predicted [22] and experimentally observed [23] to occur for strongly interacting particles placed in ac-driven two-well optical lattices. Correlated tunneling has also been studied in a driven triple-well potential [24]. Further, interaction-shifted tunneling resonances have been observed in a strongly correlated Bose gas on which frequency-doubled peaks appear as a result of next-nearest-neighbor hopping of single particles [25]. A photonic realization of the BO frequency doubling has been proposed [26,27] and experimentally achieved in waveguide lattices [28].

Unidirectional transport and super-BOs can be induced when wave packets are driven by superposed static and harmonic fields [29–35]. It is achieved when the harmonic field is resonant with the underlying BO frequency, which depends linearly on the strength of the static field. A small

detuning from the resonant condition results in super-BOs due to an effective tunneling renormalization [36]. This phenomenology has been experimentally demonstrated in a weakly interacting Bose-Einstein condensate of Cs atoms placed in a tilted optical lattice under forced driving, achieving matter-wave transport over macroscopic distances [31]. It has been theoretically demonstrated that some features of super-BOs and unidirectional transport require an important phase correction to be included in the tunneling renormalization picture [33]. Further, it has been theoretically shown that correlated super-BO of a bounded two-particle state can be observed under appropriate drive conditions [35]. Considering that the current stage of experiments is in a position to probe the effect of interactions on the driven transport of few correlated cold atoms [31], it is of fundamental importance to devise new schemes to generate and manipulate atomic entangled states in discrete lattices which can be used to probe quantum aspects of matter waves [37–39].

In this paper, we show that two interacting particles placed in a tilted optical lattice can be coherently transported when an external harmonic field is made resonant with the doubled BO frequency. We also unveil the dependence of the wave-packet centroid velocity on the strength of the interaction as well on the relative phase of the harmonic field. In contrast with the corresponding unidirectional transport for the resonant condition at the fundamental BO frequency, the degree of entanglement will be shown to continuously increase, with the particles developing positive spatial correlations due to the suppression of unbounded wave-packet components in the entire range of reachable drift velocities.

## II. MODEL AND METHODOLOGY

The dynamics of two interacting particles placed in a linear discrete lattice of spacing  $d$  under the action of superposed static dc and harmonic ac fields can be described in the framework of the tight-binding Hubbard model Hamiltonian

\*marcelo@fis.ufal.br

as [21]

$$H = \sum_{n,\sigma=1,2} [J(\hat{b}_{n+1,\sigma}^\dagger \hat{b}_{n,\sigma} + \hat{b}_{n,\sigma}^\dagger \hat{b}_{n+1,\sigma}) + eF(t)dn\hat{b}_{n,\sigma}^\dagger \hat{b}_{n,\sigma}] + \sum_n U\hat{b}_{n,1}^\dagger \hat{b}_{n,1} \hat{b}_{n,2}^\dagger \hat{b}_{n,2}, \quad (1)$$

where  $\hat{b}_{n,\sigma}$  and  $\hat{b}_{n,\sigma}^\dagger$  are the annihilation and creation operators for particles of charge  $e$  at site  $n$  in spin state  $\sigma$ ,  $J$  is the hopping amplitude, and  $U$  is the on-site Hubbard interaction. Hereafter, we consider  $U > 0$  corresponding to a repulsive Hubbard interaction. Also, we restrict ourselves to the case of  $J > 0$ . For negative  $J$  all results we report remain the same except for an overall change of sign in the wave-packet velocity. We consider the particles distinguishable by their spin state. In what follows we use units of  $e = d = J = \hbar = 1$ . The applied field is assumed to be given by  $F(t) = F_0 + F_\omega \cos(\omega t + \phi)$ . In the absence of interaction, unidirectional transport occurs when the harmonic field is resonant with the fundamental BO frequency  $\omega_B = F_0$  and its submultiples [33].

We solved the time-dependent Schrödinger equation by expanding the wave vector in the Wannier representation,  $|\Psi(t)\rangle = \sum_{n_1, n_2} \psi_{n_1, n_2}(t)|n_1, n_2\rangle$ , and followed the time evolution of an initial nonentangled Gaussian wave packet,

$$\langle n_1, n_2 | \Psi(t=0) \rangle = \frac{1}{A} e^{-[(n_1 - n_1^0)^2 + (n_2 - n_2^0)^2] / 4\sigma^2}, \quad (2)$$

centered at the initial position  $(n_1^0, n_2^0)$ .  $A$  is a normalization factor. In the following numerical results, we consider initial wave packets with  $\Sigma = 4\sigma^2 = 10$  and  $20$  and field strengths  $F_0 = 0.6$  and  $F_\omega = 0.8F_0$  [31,34]. It is important to stress that no net displacement of the wave-packet centroid is achieved for an initial Fock state with the particles occupying a single site [8]. In this case, the wave-packet dynamics is symmetric with respect to the initial position.

### III. RESULTS AND DISCUSSION

We start following the time evolution of the wave-packet centroid associated with each particle defined as

$$\langle n_i(t) \rangle = \sum_{n_1, n_2} \langle n_i | \psi_{n_1, n_2}(t) \rangle^2, \quad i = 1, 2. \quad (3)$$

Due to the symmetry of the initial state and interaction Hamiltonian, one has that  $\langle n_1(t) \rangle = \langle n_2(t) \rangle$ . In Fig. 1 we plot the centroid evolution for both cases of the ac field resonant with the fundamental and doubled BO frequencies for an intermediate interaction strength. A net unidirectional modulated motion of the wave-packet centroid is obtained, whose average velocity depends on the relative phase of the ac field.

As shown in Fig. 1, phase control of the ac field allows us to tune both the speed and the direction of the centroid motion. Within a semiclassical description, the wave-packet net velocity of a noninteracting particle driven by an ac field in resonance with the BO is given by [34]

$$v = 2J_1(F_\omega/F_0) \cos[(F_\omega/F_0) \cos \phi - \phi], \quad (4)$$

where  $J_1(x)$  is the Bessel function of the first kind of order 1. The above equation holds for the tight-binding model with only

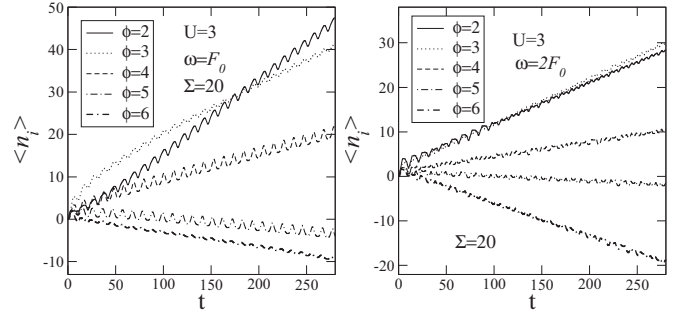


FIG. 1. Time evolution of the average position of particle 1. The ac and dc fields satisfy the resonance conditions  $\omega = F_0$  (one-particle BO frequency; left) and  $\omega = 2F_0$  (correlated BO frequency; right). Results for distinct phases  $\phi$  of the ac field are shown to stress the phase dependence of the asymptotic centroid velocity.

nearest-neighbor hopping but can be directly extended to allow for hopping processes to further sites. In Fig. 2, we plot the phase dependence of the average centroid velocity for the case of interacting particles driven by a resonant ac field. The phase dependence converges to the above semiclassical prediction as the initial wave packet becomes wider, although presenting distinct overall amplitudes and reversed trends for the cases of resonance with the fundamental and doubled BO frequencies: higher (lower) velocities are reached for wider initial wave packets at the fundamental (doubled) BO resonance. No net transport occurs for  $\phi = \pm\pi/2$ , while maximum speeds are reached at  $\phi_1 = (F_\omega/F_0) \cos \phi_1 \simeq 0.6411\dots$  (negative velocity) and  $\phi_2 = \pi - \phi_1 = 2.5008\dots$  (positive velocity).

Although the phase dependence of the drift velocity is similar to that depicted by noninteracting particles driven by an ac field resonant with the usual BO frequency, the drift velocity at the doubled BO frequency is, ultimately, an interaction effect. In the absence of interaction ( $U = 0$ ), there is no net transport at the doubled BO resonance. Unidirectional transport of a single particle can only be promoted when the frequency of the ac field is the fundamental BO frequency (or its submultiples) [33,34].

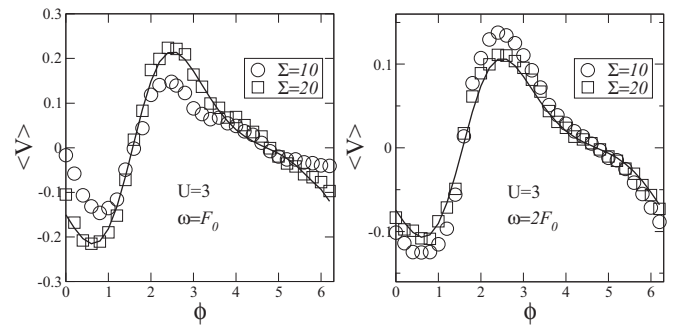


FIG. 2. Phase dependence of the one-particle centroid velocity for  $U = 3$ , with two distinct initial wave packets,  $\omega = F_0$  (left) and  $\omega = 2F_0$  (right). Solid lines correspond to the semiclassical dependence  $v \propto \cos((F_\omega/F_0) \cos \phi - \phi)$  to which the results converge as  $\Sigma \rightarrow \infty$ . Note the reversed dependence of the maximum velocity with  $\Sigma$  at the single-particle and correlated-particle resonances.

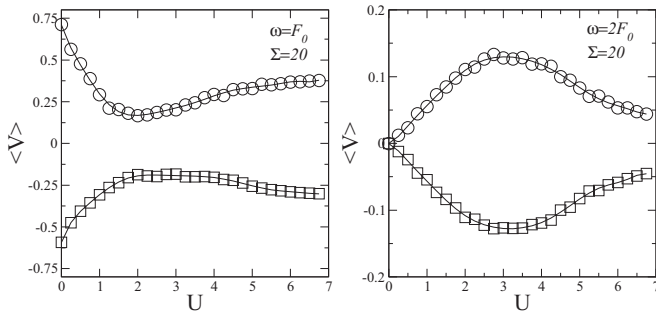


FIG. 3. Maximum one-particle drift velocity as a function of the interaction strength  $U$  for an initial wave packet with  $\Sigma = 20$ ,  $\omega = F_0$  (left), and  $\omega = 2F_0$  (right). Solid lines are guides for the eye. The interaction suppresses the maximum drift velocity when the ac field is resonant with the single-particle BOs, reaching a minimum at an intermediate value of  $U$ . The counterpart peak in the maximum drift velocity for the resonant at the doubled BO frequency reflects the predominant role played by the two-particle bounded states in this regime.

Considering that the actual value of the interparticle interaction can be tuned via the depth of optical lattices [1], we computed the extremal values of the centroid velocity as a function of  $U$  for both resonant cases (see Fig. 3). The numerical result at  $U = 0$  and  $\omega = F_0$  is consistent with the semiclassical prediction,  $v_{\max} = 2J_1(F_\omega/F_0 = 0.8) = 0.73768\dots$ , for noninteracting particles. When the interaction is turned on, the drift centroid velocity at the fundamental resonance initially decreases, reaching the minimum value at an intermediate coupling strength. On the other hand, a net transport develops at the doubled BO resonance, reaching a maximum also at a finite  $U$ . The maximum velocity reached at the correlated two-particle doubled BO resonance is of the same magnitude as the minimum drift velocity at the fundamental BO resonance. This nonmonotonous dependence of the drift centroid velocity on the coupling strength is due to two opposite effects played by the interaction in the wave-packet dynamics. The initial wave packet can be viewed as being composed of components associated with bounded and unbounded states. The unbounded wave-packet components do not drift under the action of the frequency doubled ac field. Therefore, the observed unidirectional motion of the wave-packet centroid is solely due to the drifting of the bounded wave-packet components. In these bounded states, the system behaves as a composite particle of charge  $2\varepsilon$ . Therefore, while the velocity dependence on the field frequency is the same as that of a single (although composite) particle, its nonmonotonic dependence on the interaction strength  $U$  unveils its distinct influence on bounded and unbounded states. For components associated with bounded two-particle states, the interaction favors pairing and promotes coherent hoppings. For unbounded components, the interaction enhances the wave-packet width, thus reducing the double-occupancy probability. As a result of these competing effects, optimal correlated two-particle motion occurs at an intermediate coupling strength [16]. It has been previously reported that such competition also leads to a nonmonotonic behavior of the BO amplitude [18] and Anderson localization [40,41]. It is noteworthy that bounded states also exist for

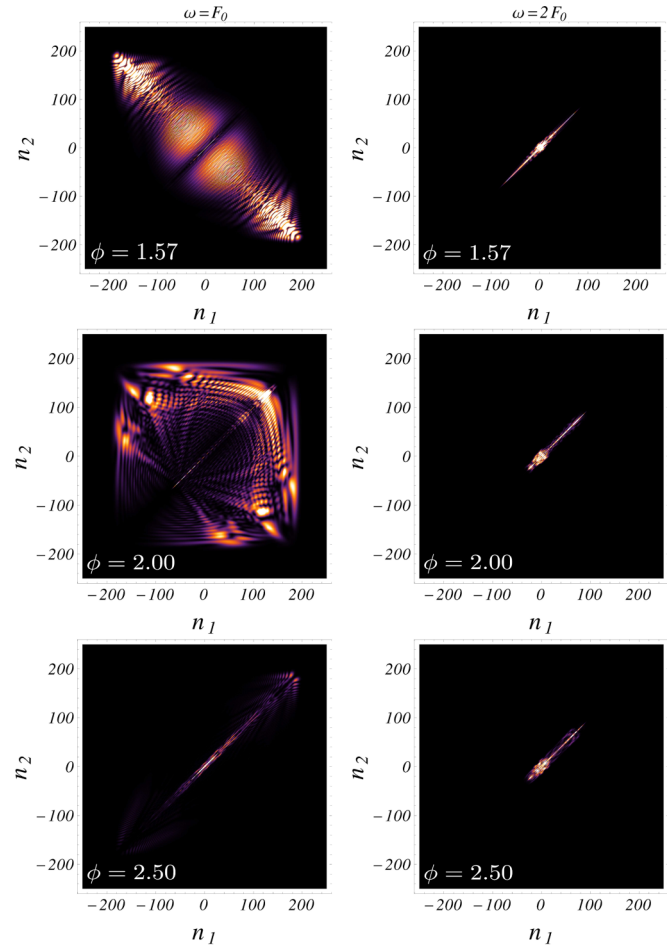


FIG. 4. Density plots of a wave packet after a finite evolution time; interaction strength  $U = 3$ . Top panels:  $\phi = \pi/2$ , for which the centroid velocity is 0. Middle panels:  $\phi = 2.0$ , leading to an intermediate velocity. Bottom panels:  $\phi = 2.5$ , resulting in the maximal velocity. Left panels: An ac field resonant with the single-particle BO ( $\omega = F_0$ ). The wave packet develops positively correlated components (the structure along the diagonal represents bounded particles) as well as anticorrelated components, with the particles being driven to opposite sides (unbounded particles), except near the maximal drift velocity. Right panels: ac field resonant with the correlated-particle BO ( $\omega = 2F_0$ ). The wave packet remains along the diagonal (bounded particles) irrespective of the phase.

negative  $U$  [42], and therefore, the above phenomenology shall remain for the case of attractive interactions.

To gain more physical insight into the wave-packet dynamics at the fundamental and doubled BO resonances, we plot in Fig. 4 some two-particle wave packets after a finite evolution time. Three representative phases of the ac field were chosen, corresponding to zero, intermediate, and maximal drift velocities. The interaction strength  $U = 3$  favors the coherent two-particle motion. At the fundamental BO resonance, the wave packet develops very distinct structures. The one along the diagonal stands for bounded states with the particles located spatially closely. The structure away from the diagonal stands for unbounded states with the particles driven to opposite sides of the chain. Only near the phase leading to the maximal drift velocity is the unbounded

component suppressed. When the ac field is resonant with the correlated two-particle doubled BO frequency, the wave packet spreads while keeping the particles spatially close for all values of the ac field phase. Under this condition, the wave packet is composed mainly of bounded two-particle states. This feature indicates that strong quantum correlations are always developed between the two particles over several lattice sites. This spatially extended quantum entangled state can be explored to probe essential quantum aspects of matter waves, such as nonlocality.

There are several prescriptions to quantify the degree of entanglement of a two-particle wave function. Here, we use as a diagnostic tool the purity function defined as  $P(t) = \text{Tr} \rho_1^2(t)$ , where  $\rho_1(t)$  is the reduced density matrix for particle 1 obtained after taking the partial trace over the states of particle 2 [ $\rho_1(t) = \text{Tr}_2 \rho(t)$ , with  $\rho(t) = |\Psi(t)\rangle\langle\Psi(t)|$ ]. From the fundamental properties of the density matrix, the purity function  $P(t) = 1$  for a pure state, meaning that the two particles are not quantum entangled. It assumes the value  $P(t) = 1/N$  whenever the quantum state of particle 1 is an even incoherent distribution among  $N$  states. In the present scenario, when the two particles become maximally quantum entangled over  $N$  lattice sites, i.e.,  $|\Psi\rangle = (1/\sqrt{N}) \sum_{i=1}^N |1 : n_i\rangle \otimes |2 : n_i\rangle$ , the partial density matrix  $\rho_1 = (1/N) \sum_{i=1}^N |1 : n_i\rangle\langle 1 : n_i|$  and the purity function reaches  $P(t) = 1/N$ . In terms of the wave-function components, the purity function can be written as

$$P = \sum_{n_1, m_1, n_2, m_2} \psi_{n_1, n_2}^* \psi_{m_1, m_2} \psi_{m_1, m_2}^* \psi_{n_1, n_2}. \quad (5)$$

As a complementary tool, we also computed the two-particle normalized correlation function, defined as

$$C(t) = [\langle n_1 n_2 \rangle - \langle n_1 \rangle \langle n_2 \rangle] / [\langle n_1 \rangle \langle n_2 \rangle]. \quad (6)$$

In Fig. 5 we show the time evolution of the purity and pair-correlation functions in the presence of an ac field resonant with the fundamental and doubled BO frequencies. When the particles are driven by an ac field at resonance with the fundamental BO frequency, the degree of entanglement saturates (although more slowly as the extremal drift velocities are approached). This saturation is related to the fact that unbounded states preponderate in the wave-packet dynamics (see Fig. 4). The component with particles driven to opposite sides of the chain has strong anticorrelations, which can surpass the positive correlation associated with the bounded components. Therefore, the net pair correlation is negative in a finite range of phase values. In contrast, the purity function continuously decreases in time when the particles are driven at resonance with the doubled BO frequency, irrespective of the phase of the ac field. This feature indicates that the wave packet develops quantum entanglement over a continuously growing chain segment for the entire range of allowed drift velocities. The positivity of the pair correlations reflects the predominant role played by bounded two-particle states. In Figs. 5(e) and 5(f) we report results for the case of initial Fock states with the particles occupying the same site, as well as separated sites. The wave-packet centroid displays no net motion in these cases [43,44]. This feature is due to the null expectation value of the kinetic operator in Fock states [44]. Even depicting no net displacement of the wave-packet

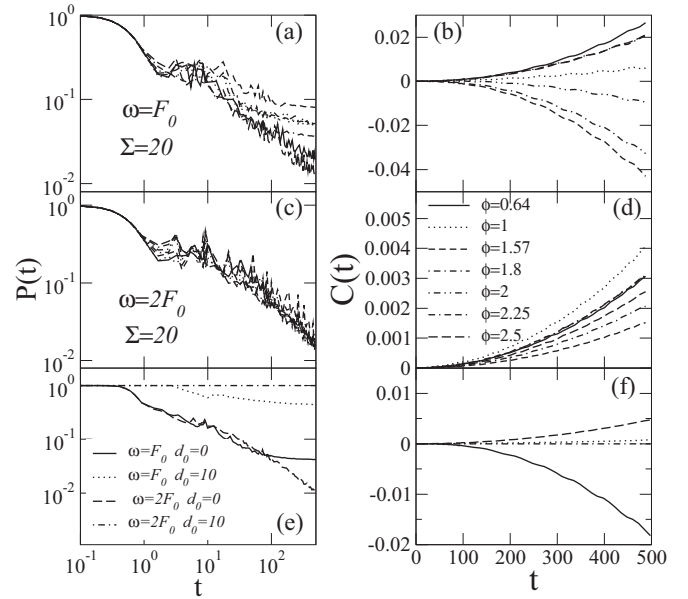


FIG. 5. Time evolution of the quantum purity function (left panels) and two-particle correlation function (right panels) for distinct phases of the ac field and  $U = 3$ . (a, b) An ac field with frequency  $\omega = F_0$ . (c, d) An ac field with frequency  $\omega = 2F_0$ . At  $\omega = 2F_0$ , the predominance of bounded states generates positive correlations and leads to an increased degree of quantum entanglement (continuously decreasing purity measure) irrespective of the phase of the ac field. (e, f) The cases of initial Fock states ( $\Sigma = 0$ ) with particles occupying the same  $d_0 = 0$  and well-separated  $d_0 = 10$  sites and field phase  $\phi = 2.5$ . Although there is no net transport, a continuously increasing degree of quantum entanglement and positive correlations is obtained only when initially close particles are driven at  $\omega = 2F_0$ .

centroid, continuously increasing quantum entanglement and positive pair correlations are still obtained for  $\omega = 2F_0$  when the particles initially occupy the same site. The generation of quantum entanglement at the frequency-doubled resonance can then be used in future experimental studies to distinguish two-particle correlated tunneling to nearest-neighbor sites from single-particle tunneling to next-nearest-neighbor sites.

#### IV. SUMMARY AND CONCLUSIONS

To conclude, we recall that recent experiments on cold atoms trapped in tilted optical lattices show the capability of observing coherent atomic motion under the action of an ac field over macroscopic distances [31,45]. Further, the coherent BO of two quantum entangled particles has also been demonstrated experimentally [1]. Therefore, the presently proposed scheme to generate and manipulate spatially extended entangled two-atom states by driving them using an ac field resonant with the frequency-doubled two-particle BO is well within currently accessible experimental techniques. The speed and direction of the wave-packet centroid motion can be externally controlled by the ac field, while the strength of the interaction can be changed by tuning the potential depth. While the phase dependence of the drift velocity is similar to that displayed by noninteracting particles driven by an ac field resonant with the usual BO frequency, its dependence

on the interaction strength  $U$  is rather nontrivial. The drift velocity vanishes in the limit of noninteracting particles and varies nonmonotonically with  $U$ , revealing the distinct roles played by unbounded- and bounded-state components on the wave-packet dynamics. Very recently, entanglement measures have been used to experimentally characterize the dynamics of strongly correlated many-body systems [39]. Although decoherence effects due to inherent coupling with other degrees of freedom must be carefully taken into account, the realization of spatially extended entangled two-atom states by exploring the phenomenon of frequency doubling of BOs

may impel the development of a new class of experiments aiming to search for signatures of quantum nonlocality in matter waves.

### ACKNOWLEDGMENTS

This work was supported by CAPES (Coordenação de Aperfeiçoamento de Pessoal de Nível Superior), CNPq (Conselho Nacional de Desenvolvimento Científico e Tecnológico), FINEP (Financiadora de Estudos e Projetos), and FA-PEAL (Fundação de Apoio à Pesquisa do Estado de Alagoas).

- 
- [1] P. M. Preiss, R. Ma, M. E. Tai, A. Lukin, M. Rispoli, P. Zupanic, Y. Lahini, R. Islam, and M. Greiner, *Science* **347**, 1229 (2015).
- [2] F. Brennecke, T. Donner, S. Ritter, T. Bourdel, M. Köhl, and T. Esslinger, *Nature* **450**, 268 (2007).
- [3] A. M. Childs, D. Gosset, and Z. Webb, *Science* **339**, 791 (2013).
- [4] A. D. Cronin, J. Schmiedmayer, and D. E. Pritchard, *Rev. Mod. Phys.* **81**, 1051 (2009).
- [5] F. Bloch, *Z. Phys.* **52**, 555 (1929).
- [6] C. Zener, *Proc. Roy. Soc. A* **145**, 523 (1934).
- [7] C. Waschke, H. G. Roskos, R. Schwedler, K. Leo, H. Kurz, and K. Köhler, *Phys. Rev. Lett.* **70**, 3319 (1993).
- [8] R. Morandotti, U. Peschel, J. S. Aitchison, H. S. Eisenberg, and Y. Silberberg, *Phys. Rev. Lett.* **83**, 4756 (1999).
- [9] M. Ben Dahan, E. Peik, J. Reichel, Y. Castin, and C. Salomon, *Phys. Rev. Lett.* **76**, 4508 (1996).
- [10] K. W. Madison, M. C. Fischer, R. B. Diener, Q. Niu, and M. G. Raizen, *Phys. Rev. Lett.* **81**, 5093 (1998).
- [11] O. Morsch, J. H. Müller, M. Cristiani, D. Ciampini, and E. Arimondo, *Phys. Rev. Lett.* **87**, 140402 (2001).
- [12] K. Bongs and K. Sengstock, *Rep. Prog. Phys.* **67**, 907 (2004).
- [13] G. Ferrari, N. Poli, F. Sorrentino, and G. M. Tino, *Phys. Rev. Lett.* **97**, 060402 (2006).
- [14] R. Battesti, P. Cladé, S. Guellati-Khélifa, C. Schwob, B. Grémaud, F. Nez, L. Julien, and F. Biraben, *Phys. Rev. Lett.* **92**, 253001 (2004).
- [15] H. Sanchis-Alepuz, Y. A. Kosevich, and J. Sanchez-Dehesa, *Phys. Rev. Lett.* **98**, 134301 (2007).
- [16] W. S. Dias, E. M. Nascimento, M. L. Lyra, and F. A. B. F. de Moura, *Phys. Rev. B* **76**, 155124 (2007).
- [17] W. S. Dias, E. M. Nascimento, M. L. Lyra, and F. A. B. F. de Moura, *Phys. Rev. B* **81**, 045116 (2010).
- [18] W. S. Dias, M. L. Lyra, and F. A. B. F. de Moura, *Phys. Lett. A* **374**, 4554 (2010).
- [19] S. Longhi and G. Della Valle, *Phys. Rev. B* **85**, 165144 (2012).
- [20] A. S. Peixoto, W. S. Dias, M. L. Lyra, and F. A. B. F. de Moura, *Physica A* **395**, 22 (2014).
- [21] R. Khomeriki, D. O. Krimer, M. Haque, and S. Flach, *Phys. Rev. A* **81**, 065601 (2010).
- [22] M. Esmann, N. Teichmann, and C. Weiss, *Phys. Rev. A* **83**, 063634 (2011).
- [23] Y. A. Chen, S. Nascimbène, M. Aidelsburger, M. Atala, S. Trotzky, and I. Bloch, *Phys. Rev. Lett.* **107**, 210405 (2011).
- [24] G. Lu, L.-B. Fu, J. Liu, and W. Hai, *Phys. Rev. A* **89**, 033428 (2014).
- [25] R. Ma, M. E. Tai, P. M. Preiss, W. S. Bakr, J. Simon, and M. Greiner, *Phys. Rev. Lett.* **107**, 095301 (2011).
- [26] S. Longhi and G. D. Valle, *Opt. Lett.* **36**, 4743 (2011).
- [27] S. Longhi, *Opt. Lett.* **36**, 3248 (2011).
- [28] G. Corrieli, A. Crespi, G. D. Valle, S. Longhi, and R. Osellame, *Nat. Commun.* **4**, 1555 (2013).
- [29] Q. Thommen, J. C. Garreau, and V. Zehnlé, *Phys. Rev. A* **65**, 053406 (2002).
- [30] V. V. Ivanov, A. Alberti, M. Schioppo, G. Ferrari, M. Artoni, M. L. Chiofalo, and G. M. Tino, *Phys. Rev. Lett.* **100**, 043602 (2008).
- [31] E. Haller, R. Hart, M. J. Mark, J. G. Danzl, L. Reichsöllner, and H.-C. Nägerl, *Phys. Rev. Lett.* **104**, 200403 (2010).
- [32] K. Kudo, T. Boness, and T. S. Monteiro, *Phys. Rev. A* **80**, 063409 (2009).
- [33] K. Kudo and T. S. Monteiro, *Phys. Rev. A* **83**, 053627 (2011).
- [34] R. A. Caetano and M. L. Lyra, *Phys. Lett. A* **375**, 2770 (2011).
- [35] S. Longhi and G. Della Valle, *Phys. Rev. B* **86**, 075143 (2012).
- [36] A. Eckardt, C. Weiss, and M. Holthaus, *Phys. Rev. Lett.* **95**, 260404 (2005).
- [37] S. Arlinghaus and M. Holthaus, *Phys. Rev. A* **84**, 063617 (2011).
- [38] O. Mandel, M. Greiner, A. Widera, T. Rom, T. W. Hansch, and I. Bloch, *Nature* **425**, 937 (2003).
- [39] R. Islam, R. Ma, P. M. Preiss, M. E. Tai, A. Lukin, M. Rispoli, and M. Greiner, *Nature* **528**, 77 (2015).
- [40] W. S. Dias and M. L. Lyra, *Physica A* **411**, 35 (2014).
- [41] C. Lee, A. Rai, C. Noh, and D. G. Angelakis, *Phys. Rev. A* **89**, 023823 (2014).
- [42] K. Winkler, G. Thalhammer, F. Lang, R. Grimm, J. H. Denschlag, A. J. Daley, A. Kantian, H. P. Büchler, and P. Zoller, *Nature* **441**, 853 (2006).
- [43] D. H. Dunlap and V. M. Kenkre, *Phys. Rev. B* **34**, 3625 (1986).
- [44] T. Hartmann, F. Keck, H. J. Korsch, and S. Mossmann, *New J. Phys.* **6**, 2 (2004).
- [45] A. Alberti, V. V. Ivanov, G. M. Tino, and G. Ferrari, *Nat. Phys.* **5**, 547 (2009).